Heterogeneous Reactions of SO_2 with HOCl and HOBr on Ice Surfaces

Ronghua Jin and Liang T. Chu*

Wadsworth Center, New York State Health Department and Department of Environmental Health Sciences, State University of New York at Albany, P.O. Box 509, Albany, New York 12201-0509, and Department of Chemistry, Shanghai Normal University, Shanghai 200234, China

Received: March 22, 2006; In Final Form: May 10, 2006

The heterogeneous reactions of SO_2 + HOX (X = Cl or Br) → products on ice surfaces at low temperature have been investigated in a flow reactor coupled with a differentially pumped quadrupole mass spectrometer. Pseudo-first-order loss of SO_2 over the ice surfaces has been measured under the conditions of concurrent HOX flow. The initial uptake coefficient of SO_2 reaction with HOX has been determined as a function of HOX surface coverage, θ_{HOX}, on the ice. The initial uptake coefficients increase as the HOX coverage increases. The uptake coefficient can be expressed as $\gamma_t = k_h\theta_{HOX}$, where k_h is an overall rate constant of SO_2 + HOCl, which was determined to be $(2.3 \pm 0.6) \times 10^{-19}$ and $(1.7 \pm 0.5) \times 10^{-19}$ molecules^{-1}·cm^2 at 190 and 210 K, and k_h of SO_2 + HOBr is $(6.1 \pm 2.0) \times 10^{-18}$ molecules^{-1}·cm^2 at 190 K. θ_{HOX} is in the range $8.1 \times 10^{13}-9.1 \times 10^{14}$ molecules·cm^{-2}. The kinetic results of the heterogeneous reaction of SO_2 + HOX on ice surface are interpreted using the Eley−Rideal mechanism. The activation energy of the heterogeneous reaction of SO_2 with HOCl on ice surface was determined to be about -37 ± 10 kJ/mol in the 190−238 K range.

I. Introduction

The chemistry of small chlorine-containing compounds, such as $ClONO_2$, on ice surfaces has received a great deal of attention in the past decade, since the discovery that these photochemically inactive compounds are involved in stratospheric ozone depletion.[1−3] Recently, considerable attention has been focused on the role of chemistry of chlorine and bromine in the marine boundary layer (MBL).[4−10] Chlorine and bromine in the MBL can affect the concentrations of ozone, hydrocarbons, and cloud condensation nuclei.

Sulfur dioxide is a pollutant in the atmosphere. The fate of SO_2 in the atmosphere is of importance, given that the SO_2 oxidation products are precursors for aerosol and cloud formation. Atmospheric SO_2 can be oxidized by OH radicals in the gas phase. It also can be oxidized by H_2O_2, O_3, and oxidants dissolved in cloud droplets, and it is eventually converted to sulfate in the form of acid rain and snow, which reach the ground as precipitates.[11] The S(IV) oxidation in the condensed phase can be significant under a variety of conditions. Field measurements have shown that the concentration of sulfate in freshly fallen snow is higher than would be expected from particulate sulfate scavenging.[12,13] Such a result is pertinent to the questions of how gaseous SO_2 enters snow ice by uptake, and how SO_2 undergoes oxidation processes.

The mean SO_2 concentration over the Atlantic is $0.24^{+0.98}_{-0.24}$ ppbv.[14] SO_2 can be taken up by snow ice, and by sea-salt aerosol, and adsorbed SO_2 is readily oxidized.[14−16] Several groups have studied the SO_2 interaction with ice.[17−20] Valdez et al. found that SO_2 is efficiently converted to S(VI) in snow samples in the field, with over 90% of the SO_2 loss due to reaction at about 271 K.[15] Laboratory experiments have confirmed that a reaction occurs between the SO_2 and H_2O_2 in the presence of ice, over a temperature range of 263−273 K.[21,22] Recently, the interaction of SO_2 with both water-ice and H_2O_2-treated ice surfaces has been investigated at lower temperature.[23,24] Chu et al. demonstrated that SO_2 loss on 0.8−3.0 wt % H_2O_2-ice is significantly higher than that on water-ice film at 190 K; and they also showed that sulfate is a major product of the reaction.[23]

Halogen compounds have significant impact on the chemistry of the boundary layer. HOX (X = Cl or Br) are major halogen-containing compounds in the MBL. HOX has been shown to oxidize S(IV) in solution,[25−27] and atmospheric chemistry modeling calculations suggested that nearly 40% of S(IV) scavenged by sea-salt aerosols is oxidized by HOCl, and a further ∼20% by HOBr, in the remote MBL.[28] The modeling calculation, which was based on the aqueous phase rate constants, indicated that the pathway accounts for the oxidation of up to 60% of S(IV) in the boundary layer by HOCl and HOBr in the pH range of 5.5−7.[28,29] The atmospheric model suggests that HOCl and HOBr are generally more important than H_2O_2 or O_3 in the oxidation of S(IV) in sea-salt aerosols in the cloud-free MBL.[30] Deliquescent sea-salt particles contain mainly Cl^- and Br^-; the chloride-to-bromide ratio is approximately 660:1, and HOX molecules scavenge from the particles with the reaction HOX + Y^- ↔ XY + OH^- (X, Y = Cl or Br).[31] Water-ice and sea-salt ice are important particulates in the MBL, and atmospheric concentrations of SO_2 (0.24 ppbv),[14] HOCl (∼0.5 ppbv),[32] and HOBr (0.26 ppbv)[33] are comparable. Presumably, reactions between SO_2 and HOX are important in the MBL; thus, the most suitable approach is to investigate the SO_2 reaction with HOX on water-ice surfaces to test whether SO_2 oxidation by HOCl is a significant pathway in the MBL. Recently, we investigated the uptake of SO_2 on HOBr-treated ice surfaces and found that uptake of SO_2 on HOBr-treated ice is significantly enhanced at 191 K.[34] However, the uptake coefficient depends strongly on the temperature within the 190−230 K range. It is uncertain how rapidly HOCl molecules can oxide SO_2 on snow/ice particle surfaces. This gap in our understanding motivated us to study the heterogeneous reaction of SO_2 with

* To whom correspondence should be addressed. E-mail: lchu@albany.edu.

10.1021/jp061796c CCC: $33.50
Published on Web 06/17/2006

HOCl on ice surfaces at low temperatures, and to assess the reaction pathway and importance of S(IV) oxidation in the boundary layer.

In the present paper, we report measurements of the uptake coefficient for the SO_2 reaction with HOCl or HOBr on water-ice surfaces under concurrent flow conditions at 190−238 K. In the sections below, we briefly describe the experimental procedures used in the determination of the uptake coefficient. We present the determinations of the initial uptake coefficient for the SO_2 reaction with HOCl on water-ice surfaces as a function of HOCl surface coverage (uptake amount) and ice film temperature, and results are then compared with values for SO_2 uptake on HOBr-ice films. The reaction pathway is discussed.

II. Experimental Section

The measurements of the uptake coefficient for the SO_2 reaction with HOX on an ice surface were performed in a flow reactor coupled to a differentially pumped quadrupole mass spectrometer (QMS). The flow-tube reactor and QMS vacuum system were interfaced with a flexible stainless steel bellows and were separated by a valve. The details of the apparatus have been discussed in our previous publications,[31,35,36] but we provide a brief description and some modifications in the present paper.

2.1. Flow Reactor. The cylindrical flow reactor was made of Pyrex glass with an inner diameter of 1.70 cm and a length of 35 cm. The outer jacket was a vacuum layer to maintain the temperature of the reactor. The temperature of the reactor was regulated by a liquid nitrogen cooled methanol circulator (Neslab) and was measured with a pair of J-type thermocouples located in the middle and at the downstream end of the reactor. During the experiment, the temperature was maintained at 190−238 K, and the stability of the temperature was better than ±0.3 K in every experiment. The total pressure inside the flow reaction chamber was controlled by a downstream throttle valve (Model 651C; MKS Instruments), and was measured by a high-precision Baratron pressure gauge (690A; MKS Instruments). The stability of the pressure was better than 0.007 Torr in every experiment. A double capillary Pyrex injector was used to admit HOX, He-water vapor, and SO_2 into the flow reactor. To avoid the water vapor condensation in the capillary at low temperature, we passed room-temperature dry air through the outside of the capillary, to keep it warm.

2.2. Water−Ice Film Preparation. The water-ice film was prepared by passing helium carrier gas (BOC; 99.9999%) through a high purity distilled water (Millipore Milli-Q Plus; >18 MΩ cm) reservoir. The reservoir was maintained at 293.15 ± 0.1 K by a refrigerated circulator (RTE-100LP; Neslab). Helium saturated with the water vapor was introduced to an inlet of the double-capillary injector. During the course of the water-ice deposition, the double-capillary injector was slowly pulled out from the downstream to the upstream at a constant speed, and a uniform ice film was deposited on the inner surface of the reactor, which was held at the temperature of the specific experiment. The amount of ice deposited was calculated from the water vapor pressure, the mass flow rate of the helium-water mixture (as measured by a Hasting mass flow meter), and the deposition time. The average film thickness, h, was calculated from the geometric area of the film on the flow reactor, the mass of ice, and the bulk density ($\rho_b = 0.63$ g/cm^3) of vapor-deposited water ice.[37] The average film thickness was about 3.3 ± 0.2 μm at 190 K, and 7.5 ± 0.2 μm at 210 K. In addition to raising the total pressure in the reactor, we prepared a thicker film on the wall of the flow reactor, and an additional section of ice was deposited in the upstream end to compensate for the migration of a small amount of ice (10^{-3} mg/h at 190 K) from the upstream end to the downstream end at a warmer temperature in each experiment; thus, the ice-film loss was minimized at warmer temperatures.

2.3. SO_2−He Mixtures. The SO_2−He mixture was prepared by mixing SO_2 (Linde; 99.98%) and helium in a glass manifold, which had been previously evacuated to ~10^{-6} Torr. SO_2 was a high purity commercial gas and was not further purified. The typical SO_2-to-He mixing ratio was 10^{-4} to 10^{-6}. The SO_2−He mixture along with additional helium carrier gas was introduced into the flow reactor via the glass and PFA tubing. The tubing was passivated by the SO_2−He mixture to establish equilibrium, as monitored by the QMS prior to every experiment. The amount of the SO_2−He mixture was controlled by two stainless steel metering valves in series, and the flow-rate was determined from the pressure change per minute in the manifold. The relationship between the flow-rate and SO_2 pressure change in the manifold was determined in a separate experiment. The total pressure change in the manifold was several Torr out of ~500 Torr during an experiment; thus, we could maintain a constant flow-rate during the experiment.

2.4. HOCl Preparation and Calibration. We previously prepared the HOCl solution by mixing NaOCl solution with $MgSO_4$ solution,[31,38,39] but we found that HOCl yield was low. We modified the synthesis method by using NaOCl and $AgNO_3$. A 15 mL aliquot of NaOCl solution (6% active chlorine; Aldrich) was diluted with the distilled water to 50 mL. An $AgNO_3$ solution (2.5 g $AgNO_3$ dissolved in 50 mL distilled H_2O) was added to the diluted NaOCl solution, drop by drop in the dark under continued stirring. The solution was then filtered, to remove precipitated AgCl. The pH value of the filtered solution was adjusted to 6.5−7.0 with diluted H_2SO_4 solution. A clear HOCl/OCl^- solution was obtained and was kept in a bubbler at 273.15 K in the dark.

Helium gas was bubbled through the HOCl solution that was maintained at 273.15 K. Both HOCl vapor and a small amount of water vapor from the HOCl solution were admitted into the reactor. The water vapor was necessary to prevent HOCl decomposition by the reaction of $2HOCl \rightarrow Cl_2O + H_2O$, during the transport of HOCl into the flow reactor. The partial water vapor pressure was controlled so as to be approximately equal to the ice vapor pressure at the ice-film temperature.

The HOCl vapor was admitted into the movable injector with PFA tubing connected by Teflon Swagelok. The flow rate was controlled by a Monel metering valve, which was treated with Halocarbon grease. The concentration of HOCl vapor was calibrated by reacting with HBr on ice surfaces at 190 K in a separate experiment.[31] In the HOCl calibration experiment, a higher concentration of HBr was admitted into the flow reactor, and the entire ice surface was exposed to HBr for about 15 min, so as to obtain sufficient surface coverage. HOCl was then introduced into the flow reactor, and it reacted with adsorbed HBr molecules to produce BrCl. Because the concentration of HBr was precisely prepared, HBr was excess in the reaction; assuming that the reaction obeyed a 1:1 stoichiometry, the loss of one HOCl molecule was equal to the formation of one BrCl molecule. Thus, we have determined the signal ratio of HOCl to BrCl by the QMS. In another experiment, HOCl was in excess, and the same experimental procedures were repeated. In this case, the loss of HBr molecules was equal to the formation of BrCl molecules. We measured the signal ratio of HBr to BrCl. From these two experiments, we determined the

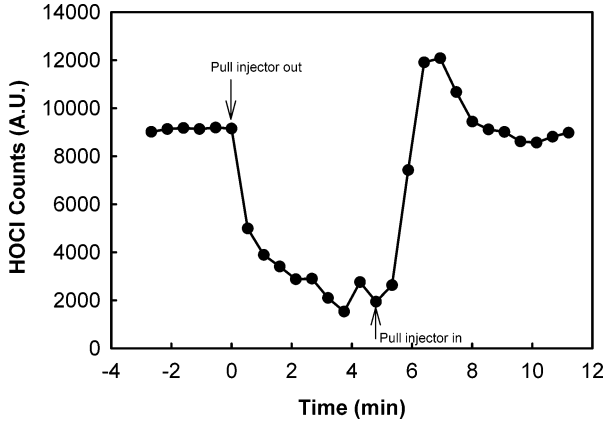

Figure 1. Uptake of HOCl on water-ice film at $P_{HOCl} = 2.7 \times 10^{-6}$ Torr and 189.5 K. (●) represents the HOCl signal. The total pressure is 1.000 ± 0.002 Torr, and the water-ice film thickness is 3.4 μm. The uptake starts at $t = 0$ min when the HOCl was exposed to the ice film; HOCl lost on the ice film immediately. The background HOCl signal was corrected. After HOCl had been exposed to the water-ice film for approximately 5 min, the injector was pushed in, and adsorbed HOCl was desorbed. Surface coverage of HOCl is $(2.5 \pm 0.4) \times 10^{14}$ molecules/cm^2. The error bar associated with each data point is approximately the size of the plotted points.

signal ratio (QMS counts) of HOCl to HBr. Knowing both the signal ratio of HOCl to HBr and the HBr QMS counts-to-concentration ratio, we have determined the gas-phase HOCl concentration.

When the HOCl molecule was exposed to the water-ice surface, it was taken up the surface immediately. A typical time course of HOCl take-up by a water-ice film at 190 K is shown in Figure 1. Figure 1 shows that HOCl is taken up by water-ice for about 5 min, for a HOCl surface coverage of $\sim(2.5 \pm 0.4) \times 10^{14}$ molecules/cm^2. Then, the injector was pushed back to the downstream end, the HOCl-ice film was heated by the injector, and a portion of adsorbed HOCl was desorbed immediately.

2.5. HOBr Preparation and Calibration. The HOBr solution was prepared by addition of bromine (Aldrich; 99.5%) drop-by-drop to an ice-cooled glass flask, in which 2.1 g of $AgNO_3$ (Baker; 99.9%) had been dissolved in 100 mL of distilled H_2O, until the orange color indicative of excess bromine persisted under continued stirring.[34,40,41] After the solution had been stirred for a further 45 min, it was filtered to remove all precipitated AgBr. The filtered solution was freed of Br_2 by six successive extractions with CCl_4, each with 20 mL of CCl_4. A slightly yellowish clear HOBr solution was obtained and was kept in a bubbler at 273.15 K in the dark.[34,42]

The concentration of HOBr vapor was calibrated by reaction of its vapor with HCl on ice surfaces at 190 K, in a separate experiment, similar to the HOCl calibration; the details can be found in our previous publications.[34,42] The HOX calibration was based on the stoichiometric ratio of the HOX + HY reaction on ice. The precision of the HOX concentration measurement was very good with a typical error of 10%; however, the accuracy of the HOX concentration also depends on a systematic error that was estimated up to ~50%.

2.6. Determination of the Uptake Coefficient. The initial uptake coefficient, γ_w, for SO_2 reaction with HOX (X = Cl or Br) on the water-ice film under the condition of concurrent flow was determined as follows. First, a 20 cm length of water-ice film was prepared by water vapor deposition on the inner wall of the flow reactor, as described in section 2.2, for every measurement. Second, the helium carrier gas was bubbled

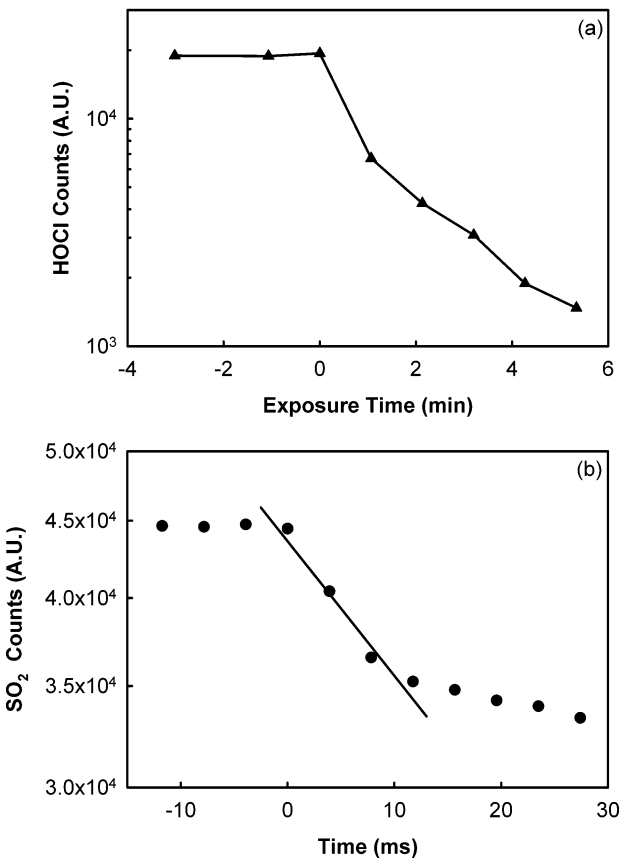

Figure 2. The reaction of SO_2 and HOCl on a water-ice film surface at 190 K. (a) Relationship between the HOCl signal loss and exposure time on a water-ice film surface. (▲) represents the HOCl signal. The plot shows the initial HOCl signal, before HOCl came in contact with water-ice ($t < 0$); the uptake, starting at $t = 0$ min, when HOCl was exposed to the ice film; and the loss of HOCl on the ice film. The background HOCl signal was corrected. The HOCl surface coverage is $(3.8 \pm 0.6) \times 10^{14}$ molecules/cm^2. (b) Relationship between the log SO_2 signal and reaction time (z/v) on water-ice. (●) represents the SO_2 QMS signal. The plot shows the initial SO_2 signal, before SO_2 came in contact with HOCl on the ice ($t < 0$), and the loss of SO_2 on the HOCl-ice film under the condition of concurrent SO_2 and HOCl flow. The background SO_2 signal was subtracted. The pseudo-first-order rate constant was determined to be $k_s = 20.4 \pm 2.0$ s^{-1}, and the corrected rate constant $k_w = 21.1 \pm 2.1$ s^{-1}. The initial uptake coefficient is $\gamma_w = (1.4 \pm 0.2) \times 10^{-3}$. $P_{HOCl} = 4.2 \times 10^{-6}$ Torr and $P_{SO_2} = 1.4 \times 10^{-6}$. The total pressure is 1.000 ± 0.002 Torr, and the water-ice film thickness is 3.3 μm. The error bars on the data points are about the size of the plotted points.

through the HOX solution, which was kept at 273.15 K. The HOX vapor−He mixture was then admitted to one inlet of the double capillary injector, and the SO_2−He mixture was admitted to the other inlet of the injector. Before SO_2 reacted with HOX on the water-ice film, both initial SO_2 and HOX signals were determined by the QMS. HOCl was monitored by the QMS at $m/e^- = 52$, HOBr at $m/e^- = 96$, and SO_2 at $m/e^- = 64$. Once both SO_2 and HOX signals were stabilized, the sliding injector was slowly pulled out toward the upstream end of the flow reactor, 2 cm at a time. A typical QMS signal for SO_2 and HOCl on a water-ice surface is shown in Figure 2. The typical data acquisition time was 10−30 s per point, and the partial pressures of HOCl (P_{HOCl}) were always maintained higher than that of P_{SO_2} during the reaction. Once the QMS sensitivity for HOCl was calibrated, the gas-phase HOCl concentration is known. The surface coverage of HOCl was determined by the integration of the calibrated HOCl signal over the exposure time (Figure 2a). The loss of SO_2 reaction with HOCl on the water-ice film

was measured by the QMS, as a function of the injector distance *z*. For the pseudo-first-order rate under plug-flow conditions, the following relationship holds for SO_2:

$$\ln [SO_2]_z = -k_s(z/v) + \ln [SO_2]_0 \quad (1)$$

where *z* is the injector position, v is the mean flow velocity, $[SO_2]_z$ is the gas-phase SO_2 concentration measured by the QMS at position *z*, and the subscript 0 is the initial injector reference position. For a typical experiment of SO_2 + HOCl performed on water-ice film at 190 K, the pseudo-first-order SO_2 loss is shown in Figure 2b. The pseudo-first-order loss rate constant, k_s, was determined from the least-squares fit of the experimental data to eq 1. A value of $k_s = 20.4 \pm 2.0\ s^{-1}$ at 190 K was obtained for SO_2 + HOCl. k_s was then corrected for gas-phase axial and radial diffusion using a standard procedure,[43] and the corrected rate constant was termed k_w. A diffusion coefficient for SO_2 in helium was estimated to be 160 $cm^2 \cdot s^{-1} \cdot Torr^{-1}$ at 190 K and 1.0 Torr.[23,44] The uptake coefficient γ_w was calculated from k_w using[39,45]

$$\gamma_w = 2Rk_w/(\omega + Rk_w) \quad (2)$$

where *R* is the radius of the flow reactor (0.85 cm) and ω is the mean SO_2 molecular velocity at the water-ice film temperature.

The typical amount of SO_2 loss to HOCl-ice surface is $\sim 10^{12-13}$ molecules/cm^2, which is a factor of approximately 10−100 lower than the corresponding amount of HOCl taken up by the ice surface in the same time period (see Figure 2). This shows that the pseudo-first-order approximation used in eq 1 is valid under the present experimental conditions.

It is generally accepted that the vapor-deposited ice film has internal surface areas and is porous. To obtain a "true" uptake coefficient γ_t, as if the film were a geometrically smooth surface, we correct γ_w for contributions from the internal porosity. On the basis of previous studies, which were conducted at similar conditions,[46,47] H_2O ice films can be approximated as hexagonally close-packed spherical granules stacked in layers.[48] The true uptake coefficient, γ_t, is related to the value γ_w, by

$$\gamma_t = \frac{\sqrt{3}\gamma_w}{\pi\{1 + \eta[2(N_L - 1) + (3/2)^{1/2}]\}} \quad (3)$$

where the effectiveness factor, η, is the fraction of the film surface that participates in the reaction and N_L is the number of granule layers.[39,48] Detailed calculations for these parameters can be found in refs 46-48. A tortuosity factor $\tau = 4$ and true ice density $\rho_t = 0.925\ g \cdot cm^{-3}$ were used in the above calculation.

III. Results

3.1. Uptake Coefficients for SO_2 on Ice Films with Various HOCl Coverages. *SO_2 on the HOCl−Ice Films.* In this experiment, a 20 cm length of ice film was vapor-deposited on the wall of the flow reactor. SO_2 and HOCl were then exposed to the freshly prepared ice surface simultaneously, as the sliding injector was slowly pulled out in even increments. The gas-phase SO_2 loss was measured by the QMS as a function of the injector distance *z*, and the HOCl loss was monitored as a function of exposure time. The typical SO_2 pressure is $(1.4 \pm 0.2) \times 10^{-6}$ Torr. The pseudo-first-order rate constant, k_s, and initial uptake coefficient, γ_w, for SO_2 reaction with HOCl on a water-ice film, were determined using eqs 1 and 2, respectively. γ_w was determined as a function of the HOCl surface coverage

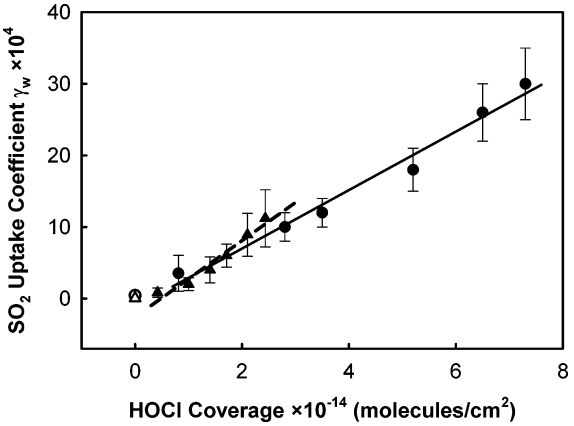

Figure 3. Relationship between the initial uptake coefficient, γ_w, and HOCl surface coverage. (●) is at 190 K and (▲) is at 210 K. The thickness of the ice film is 3.3 ± 0.2 μm at 190 K, and 7.5 ± 0.2 μm at 210 K. The partial pressure of SO_2 is $(1.4 \pm 0.2) \times 10^{-6}$ Torr, and the total pressure in the reactor is 1.000 ± 0.007 Torr. It can be seen that γ_w increases as HOCl coverage increases. Included in the plot are γ_w values of SO_2 on water-ice at 191 (○) and 210 K (△). γ_w of SO_2 reaction with HOCl is higher than γ_w of SO_2 on water-ice.

(molecules/cm^2) at 190 K and at 210 K. We varied both HOCl flow rate (5−30 sccm) and partial HOCl pressure ($P_{HOCl} = 1.5 \times 10^{-6}$−$5.1 \times 10^{-6}$ Torr), to achieve different HOCl surface coverages. Due to the nature of HOCl and ice interaction, and the constraint of the flow conditions for HOCl and SO_2, HOCl surface coverage can be varied only over a limited range. Those results are shown in Figure 3, and detailed experimental conditions are presented in Table 1. γ_w values are typically averages of two to five measurements, and every measurement was conducted on a freshly prepared ice film. The errors listed in Table 1 and the error bars in Figure 3 include both 1 standard deviation $\pm\sigma$ of the mean value and systematic errors of the pressure gauges, digital thermometers, and mass flow meters, estimated to be approximately 8%. γ_t is corrected for porosity of the ice film using eq 3. Figure 3 shows that the γ_w values increase from 3.5×10^{-4} to 3.0×10^{-3}, when the HOCl surface coverage increases from 8.1×10^{13} to 7.3×10^{14} molecules/cm^2 at 190 K. At 210 K, the initial uptake coefficient γ_w increases from 8.2×10^{-5} to 1.1×10^{-3}, as the HOCl surface coverage increases from 4.2×10^{13} to 2.4×10^{14} molecules/cm^2. In general, the initial uptake coefficients for SO_2 reaction with HOCl on water-ice film at 210 K are slightly lower than that at 191 K. The SO_2 uptake by reaction with HOCl on ice surfaces is enhanced compared to that on water-ice at both 190 and 210 K.[34]

Surface Deactivation. The γ of SO_2 + HOCl on a water-ice film decreases slightly as the number of repeated measurement increases, when SO_2 reacts with HOCl at 190.1 K (Figure 4). The initial uptake coefficient γ_w is $(1.2 \pm 0.15) \times 10^{-3}$, and subsequent γ values are $(1.0 \pm 0.14) \times 10^{-3}$, $(9.6 \pm 1.4) \times 10^{-4}$, and $(8.1 \pm 1.1) \times 10^{-4}$. This indicates that the uptake coefficient of SO_2 decreases 10−20% after each repeated measurement, and it is an indication of weak surface deactivation. The observation suggests that the surface is deactivated slightly, perhaps due to sulfate product that remains on the ice surface (see Discussion). The effect of surface deactivation on measured initial uptake coefficients is very small, because the uncertainty of measurement is comparable in magnitude with the deactivation effect.

3.2. Effect of Temperature on Initial Uptake Coefficients. We employed thicker ice films, 32 ± 1 μm, and a higher total pressure in the flow reactor, 2.000 ± 0.008 Torr, to cover wider

TABLE 1: Uptake Coefficients for the SO_2 Reaction with HOCl on Ice Surfaces at 190 K and 210K[a]

temp (K)	P_{SO_2} (Torr)	v (m/s)	HOCl uptake amount (molecules/cm^2)	k_s (1/s)	k_w (1/s)	γ_w	γ_t[b]
190.1 ± 0.6	1.5×10^{-6}	5.1	$(8.1 \pm 1.7) \times 10^{13}$	5.17 ± 3.76	5.23 ± 3.82	$(3.5 \pm 2.5) \times 10^{-4}$	1.6×10^{-5}
189.5 ± 0.4	1.4×10^{-6}	4.9	$(2.8 \pm 0.4) \times 10^{14}$	15.1 ± 2.6	15.7 ± 2.6	$(1.0 \pm 0.2) \times 10^{-3}$	4.8×10^{-5}
190.1 ± 0.3	1.4×10^{-6}	5.4	$(3.5 \pm 0.5) \times 10^{14}$	16.8 ± 2.3	17.3 ± 2.4	$(1.2 \pm 0.2) \times 10^{-3}$	5.8×10^{-5}
189.8 ± 0.5	1.4×10^{-6}	5.6	$(5.2 \pm 0.9) \times 10^{14}$	25.2 ± 3.4	26.1 ± 3.5	$(1.8 \pm 0.3) \times 10^{-3}$	9.1×10^{-5}
190.1 ± 0.4	1.4×10^{-6}	5.9	$(6.5 \pm 1.0) \times 10^{14}$	36.7 ± 5.9	38.9 ± 6.4	$(2.6 \pm 0.4) \times 10^{-3}$	1.4×10^{-4}
190.1 ± 0.5	1.3×10^{-6}	6.1	$(7.3 \pm 1.1) \times 10^{14}$	41.4 ± 6.1	44.0 ± 6.6	$(3.0 \pm 0.5) \times 10^{-3}$	1.6×10^{-4}
209.8 ± 0.3	1.5×10^{-6}	5.8	$(4.2 \pm 1.0) \times 10^{13}$	1.28 ± 1.02	1.28 ± 1.02	$(8.2 \pm 6.6) \times 10^{-5}$	2.3×10^{-6}
209.8 ± 0.8	1.6×10^{-6}	5.9	$(1.0 \pm 0.2) \times 10^{14}$	3.14 ± 1.36	3.15 ± 1.37	$(2.0 \pm 0.9) \times 10^{-4}$	5.6×10^{-6}
209.7 ± 0.5	1.5×10^{-6}	6.2	$(1.4 \pm 0.3) \times 10^{14}$	6.16 ± 2.78	6.21 ± 2.84	$(4.0 \pm 1.8) \times 10^{-4}$	1.1×10^{-5}
209.8 ± 0.5	1.4×10^{-6}	6.4	$(1.7 \pm 0.3) \times 10^{14}$	9.17 ± 2.51	9.27 ± 2.54	$(6.0 \pm 1.6) \times 10^{-4}$	1.8×10^{-5}
210.0 ± 0.3	1.4×10^{-6}	6.7	$(2.1 \pm 0.3) \times 10^{14}$	13.6 ± 4.5	13.8 ± 4.7	$(8.9 \pm 3.0) \times 10^{-4}$	2.7×10^{-5}
209.7 ± 0.4	1.3×10^{-6}	6.9	$(2.4 \pm 0.4) \times 10^{14}$	17.0 ± 6.3	17.4 ± 6.5	$(1.1 \pm 0.4) \times 10^{-3}$	3.4×10^{-5}

[a] Total pressure was 1.000 ± 0.007 Torr; H_2O-ice films thickness was 3.3 ± 0.2 μm at 190 K and 7.5 ± 0.2 μm at 210 K. [b] γ_t was calculated from eq 3 by using $N_L = 6$ at 3.3 ± 0.2 μm at 190 K; $N_L = 10$ at 7.5 ± 0.2 μm at 210 K using the data provided in ref 46 and 48.

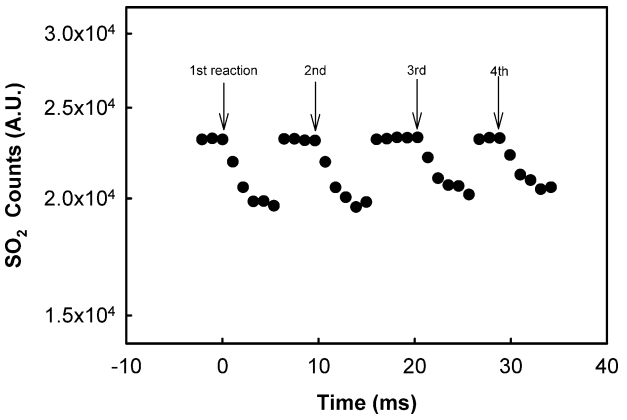

Figure 4. Plot of γ of SO_2 reaction with HOCl on a water-ice film, shown as repeated measurements at 190.1 K. The background SO_2 signal has been subtracted from the plotted values. The arrows indicate the reference position z_o of each measurement. The initial uptake coefficient γ_w is 1.2×10^{-3}. The injector was pushed back to enable subsequent measurements to be made on the same ice film. γ values are 1.0×10^{-3}, 9.6×10^{-4}, and 8.1×10^{-4}. The result suggests that a weak surface deactivation is occurring. $P_{SO_2} = 1.6 \times 10^{-6}$ Torr, $P_{HOCl} = 2.8 \times 10^{-6}$ Torr, the thickness of the ice film is 3.3 μm, and the total pressure is 1.00 Torr.

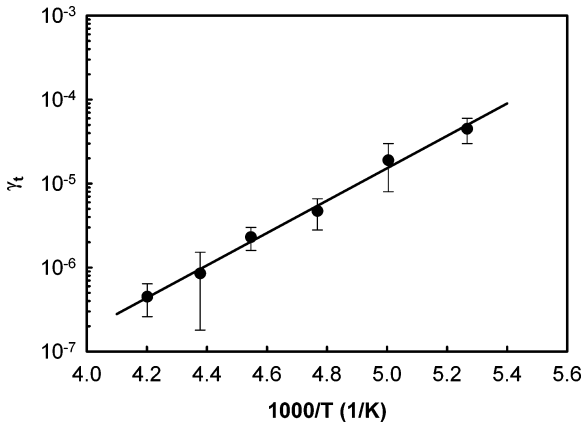

Figure 5. Relationship between the logarithm of the uptake coefficient, γ_t, of the SO_2 reaction with HOCl on water-ice surfaces and $1/T$. The solid line was fitted to the experimental data at 190−238 K using the Arrhenius equation. The activation energy E_a was determined to be about −37 ± 10 kJ/mol. $P_{SO_2} = (1.4 \pm 0.2) \times 10^{-6}$ Torr, $P_{HOCl} = (4.0 \pm 0.5) \times 10^{-6}$ Torr, and the total pressure is 2.000 ± 0.008 Torr. The water-ice film thickness is 32 ± 1 μm.

temperature ranges. The initial uptake coefficient for SO_2 reaction with HOCl on water-ice film, γ_w, decreases dramatically from 1.8×10^{-3} to 2.6×10^{-5}, as the temperature of the water-ice film increases from 190 to 238 K, whereas the partial pressure of HOCl is maintained at $(4.0 \pm 0.5) \times 10^{-6}$ Torr (Figure 5). HOCl surface coverage decrease slightly from 189 to 218 K, but it decreases further as the temperature increases to 228 K, likely due either to an increasing evaporation rate of ice at warmer temperature or else to HOCl desorption from the ice surface. Table 2 summarizes the results. γ_t is corrected for the ice film porosity. The activation energy E_a for SO_2 reaction with HOCl on a water-ice surface was calculated from the slope of the plot of log γ_t versus $1/T$ at 190−238 K. E_a was determined to be about −37 ± 10 kJ/mol (see details in section 4.3).

3.3. Uptake Coefficients for SO_2 on Ice Films with Various HOBr Coverages. A 20 cm length of ice film was vapor-deposited on the wall of the flow reactor. SO_2 and HOBr were concurrently exposed to a freshly prepared ice surface, as the sliding injector was slowly pulled out incrementally toward the upstream end. The amount of HOBr taken by the ice film was determined by the QMS. Again, both HOBr flow-rate (4−20 sccm) and partial HOBr pressure ($P_{HOBr} = 1.8 \times 10^{-6}$−$6.6 \times 10^{-6}$ Torr) were varied to achieve a range of surface coverages. The gas-phase loss of SO_2, at a pressure of $(1.5 \pm 0.2) \times 10^{-6}$ Torr, was measured by the QMS, as a function of the injector distance z. The pseudo-first-order rate constant, k_s, and initial uptake coefficient, γ_w, for SO_2 reaction with HOBr on water-ice film surfaces were determined from eqs 1 and 2. γ_w was measured as a function of the HOBr surface coverage at 190 K. The results are shown in Figure 6, and detailed experimental conditions are presented in Table 3. γ_t is corrected for porosity of the ice using eq 3. Figure 6 shows that the γ_w values increase from 5.2×10^{-3} to 2.7×10^{-2}, when the HOBr surface coverage increases from 2.6×10^{14} to 9.1×10^{14} molecules/cm^2 at 190 K. At a given surface coverage, 5×10^{14} molecules/cm^2, the initial uptake coefficient of SO_2 on HOBr-ice is approximately 1 order of magnitude higher than that on HOCl-ice at 190 K.

IV. Discussion

4.1. Uptake Coefficients of SO_2 Reaction with HOX on Water−Ice Films. The initial uptake coefficients of SO_2 were measured as a function of the HOCl surface coverage, at 190 and 210 K (Figure 3), and as a function of the HOBr surface coverage at 190 K (Figure 6). γ_w was then corrected for the ice porosity using eq 3. The steady-state SO_2 uptake amount on water-ice is 2.4×10^{12} molecules/cm^2 at 191 K, and the uptake coefficient γ_t is $\sim 5 \times 10^{-7}$.[23] The uptake coefficient of HOCl ($\gamma_t = 6.9 \times 10^{-4}$) on the water-ice surface is orders of magnitude higher than that of SO_2 and the surface coverage

TABLE 2: Uptake Coefficients for the SO_2 Reaction with HOCl on Ice Surfaces at Varying Temperature[a]

temp (K)	P_{SO_2} (Torr)	v (m/s)	HOCl uptake amount (molecules/cm^2)	k_s (1/s)	k_w (1/s)	γ_w	γ_t[b]
189.9 ± 0.4	1.5×10^{-6}	2.6	$(2.5 \pm 0.4) \times 10^{14}$	23.8 ± 4.6	25.8 ± 5.1	$(1.8 \pm 0.4) \times 10^{-3}$	$(4.5 \pm 1.5) \times 10^{-5}$
199.8 ± 0.5	1.5×10^{-6}	2.7	$(2.4 \pm 0.5) \times 10^{14}$	13.2 ± 7.0	13.9 ± 7.5	$(9.2 \pm 4.1) \times 10^{-4}$	$(1.9 \pm 1.1) \times 10^{-5}$
209.7 ± 0.3	1.3×10^{-6}	2.8	$(1.6 \pm 0.3) \times 10^{14}$	3.92 ± 1.47	3.97 ± 1.51	$(2.6 \pm 1.0) \times 10^{-4}$	$(4.7 \pm 1.9) \times 10^{-6}$
218.0 ± 0.3	1.3×10^{-6}	2.9	$(1.2 \pm 0.2) \times 10^{14}$	2.06 ± 0.69	2.08 ± 0.71	$(1.3 \pm 0.4) \times 10^{-4}$	$(2.3 \pm 0.7) \times 10^{-6}$
228.4 ± 0.7	1.3×10^{-6}	3.0	$(4.8 \pm 2.4) \times 10^{13}$	0.78 ± 0.62	0.78 ± 0.63	$(4.9 \pm 3.8) \times 10^{-5}$	$(8.5 \pm 6.7) \times 10^{-7}$
238.0 ± 1.1	1.3×10^{-6}	3.1	$(2.5 \pm 1.1) \times 10^{13}$	0.42 ± 0.21	0.42 ± 0.21	$(2.6 \pm 1.1) \times 10^{-5}$	$(4.5 \pm 1.9) \times 10^{-7}$

[a] Total pressure was 2.000 ± 0.008 Torr; H_2O-ice film thickness was 32 ± 1μm; P_{HOCl} was $(4.0 \pm 0.5) \times 10^{-6}$ Torr. [b] γ_t was calculated from eq 3 by using $N_L = 16$.[48]

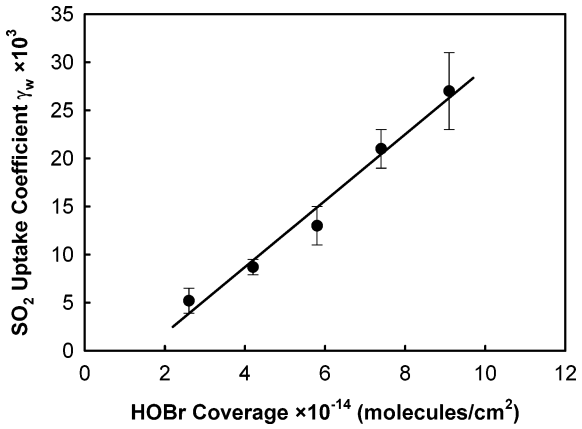

Figure 6. Relationship between the initial uptake coefficient of SO_2, γ_w, and HOBr surface coverage. (●) is γ_w on water-ice films at 190 K. The thickness of the ice film is 3.5 ± 0.2 μm at 190 K. The partial pressure of SO_2 is $(1.5 \pm 0.2) \times 10^{-6}$ Torr, and the total pressure in the reactor is 1.000 ± 0.007 Torr. The plot indicates that γ_w increases as HOBr coverage increases. The solid line is drawn as a visual aid.

for HOCl can be up to 10^{14} molecule/cm^2. These facts suggest that the interaction between HOCl and water-ice surfaces is stronger than that between SO_2 and ice at 190 K. On the basis of this work and our previous work,[34] we deduce that HOCl is adsorbed on the ice, and that incoming SO_2 reacts with adsorbed HOCl (Eley−Rideal mechanism). The reaction between SO_2 and HOBr follows the same pathway:

$$\mathrm{HOX(g)} \underset{k_{-1}}{\overset{k_1}{\rightleftharpoons}} \mathrm{HOX(ad)} \tag{4}$$

$$\mathrm{HOX(ad)} \underset{k_{-2}}{\overset{k_2}{\rightleftharpoons}} \mathrm{H^+ + OX^-(ad)} \tag{5}$$

$$\mathrm{SO_2(g) + HOX(ad)} \underset{k_{-3}}{\overset{k_3}{\rightleftharpoons}} \mathrm{[HOX\cdots SO_2(ad)]} \xrightarrow{k_4} \mathrm{product} \tag{6}$$

$$\mathrm{SO_2(g) + OX^-(ad)} \underset{k_{-5}}{\overset{k_5}{\rightleftharpoons}} \mathrm{[XO^-\cdots SO_2(ad)]} \xrightarrow{k_6} \mathrm{product} \tag{7}$$

where X = Cl or Br. The observed gas-phase SO_2 loss rate can be written as

$$-\frac{\mathrm{d[SO_2(g)]}}{\mathrm{d}t} = k_3[\mathrm{SO_2(g)}][\mathrm{HOX(ad)}] - k_{-3}[\mathrm{HOX\cdots SO_2(ad)}] + k_5[\mathrm{SO_2(g)}][\mathrm{OX^-(ad)}] - k_{-5}[\mathrm{XO^-\cdots SO_2(ad)}] \tag{8}$$

where $[SO_2(g)]$ is the SO_2 concentration. We apply the steady-state approximation to $[HOX\cdots SO_2(ad)]$ and $[OX^-\cdots SO_2(ad)]$, i.e., $d[HOX\cdots SO_2(ad)]/dt = 0$ and $d[OX^-\cdots SO_2(ad)]/dt = 0$, and then substitute the result into eq 8. We have

$$-\frac{\mathrm{d[SO_2(g)]}}{\mathrm{d}t} = \frac{k_3k_4}{k_{-3}+k_4}[\mathrm{SO_2(g)}][\mathrm{HOX(ad)}] + \frac{k_5k_6}{k_{-5}+k_6}[\mathrm{SO_2(g)}][\mathrm{XO^-(ad)}] \tag{9}$$

Equation 9 can be expressed as

$$-\frac{\mathrm{d[SO_2(g)]}}{\mathrm{d}t} = \frac{k_{HOX}[H^+] + k_{OX^-}K_2}{K_2 + [H^+]}[\mathrm{SO_2(g)}][\mathrm{HOX(ad)}]_T \tag{10}$$

where

$$k_{HOX} = \frac{k_3k_4}{k_{-3}+k_4} \qquad k_{OX^-} = \frac{k_5k_6}{k_{-5}+k_6}$$

$$[\mathrm{HOX(ad)}]_T = [\mathrm{HOX(ad)}] + [\mathrm{XO^-(ad)}] = \theta^T_{HOX}$$

$$\text{and } K_2 = \frac{k_2}{k_{-2}} = \frac{[H^+][XO^-]}{[HOX]}$$

The uptake coefficient γ_t of SO_2 can be expressed as

$$\gamma_t = \frac{-\dfrac{\mathrm{d[SO_2(g)]}}{\mathrm{d}t}}{\dfrac{[\mathrm{SO_2(g)}]\omega}{4}} = \frac{4(k_{HOX}[H^+] + k_{OX^-}K_2)}{\omega(K_2 + [H^+])}\theta^T_{HOX} \tag{11}$$

where ω is the mean molecular velocity of SO_2, and $\theta^T_{HOX} = \theta_{HOX} + \theta_{OX^-}$ is the total HOX surface coverage on the ice surface. Equation 11 indicates that γ_t is proportional to the total HOX surface coverage. It explains the experimental data (Figures 3 and 6) well: as HOX coverage increases, the initial uptake coefficient increases. We can also express eq 11 as

$$\gamma_t = k_h\theta^T_{HOX} \tag{12}$$

where $k_h = 4(k_{HOX}[H^+] + k_{OX^-}K_2)/\omega(K_2 + [H^+])$, an overall rate constant, is the combination of all rate constants and conversion factors. The experimental data, γ_t, were fitted to eq 12; the results for the SO_2 reaction with HOCl are shown in Figure 7a, and the results for SO_2 reaction with HOBr are shown in Figure 7b. The overall rate constant k_h of SO_2 reaction with HOCl was determined from the slope of the fit to be $(2.3 \pm 0.6) \times 10^{-19}$ and $(1.7 \pm 0.5) \times 10^{-19}$ molecules^{-1}·cm^2, at 190 and 210 K, respectively, and the overall rate constant k_h of SO_2 reaction with HOBr was $(6.1 \pm 2.0) \times 10^{-18}$ molecules^{-1}·cm^2 at 190 K. The fitted line represents the experimental results well, suggesting that the simple model represents a possible reaction pathway. Examining k_h values, we can conclude that γ_t of SO_2

TABLE 3: Uptake Coefficients for the SO_2 Reaction with HOBr on Ice Surfaces[a]

temp (K)	P_{SO_2} (Torr)	v (m/s)	HOBr uptake amount (molecules/cm^2)	k_s (1/s)	k_w (1/s)	γ_w	γ_t
190.0 ± 0.3	1.5×10^{-6}	4.8	$(2.6 \pm 0.5) \times 10^{14}$	68 ± 16	77 ± 19	$(5.2 \pm 1.3) \times 10^{-3}$	3.3×10^{-4}
190.1 ± 0.4	1.6×10^{-6}	5.0	$(4.2 \pm 0.8) \times 10^{14}$	107 ± 11	129 ± 12	$(8.7 \pm 0.8) \times 10^{-3}$	6.9×10^{-4}
190.1 ± 0.3	1.5×10^{-6}	5.3	$(5.8 \pm 0.7) \times 10^{14}$	152 ± 14	198 ± 19	$(1.3 \pm 0.2) \times 10^{-2}$	1.3×10^{-3}
190.2 ± 0.3	1.5×10^{-6}	5.5	$(7.4 \pm 1.1) \times 10^{14}$	215 ± 19	316 ± 29	$(2.1 \pm 0.2) \times 10^{-2}$	2.8×10^{-3}
190.1 ± 0.4	1.5×10^{-6}	5.6	$(9.1 \pm 1.3) \times 10^{14}$	255 ± 27	411 ± 51	$(2.7 \pm 0.4) \times 10^{-2}$	4.2×10^{-3}

[a] Total pressure was 1.000 ± 0.007 Torr; H_2O-ice film thickness was 3.5 ± 0.2 μm.

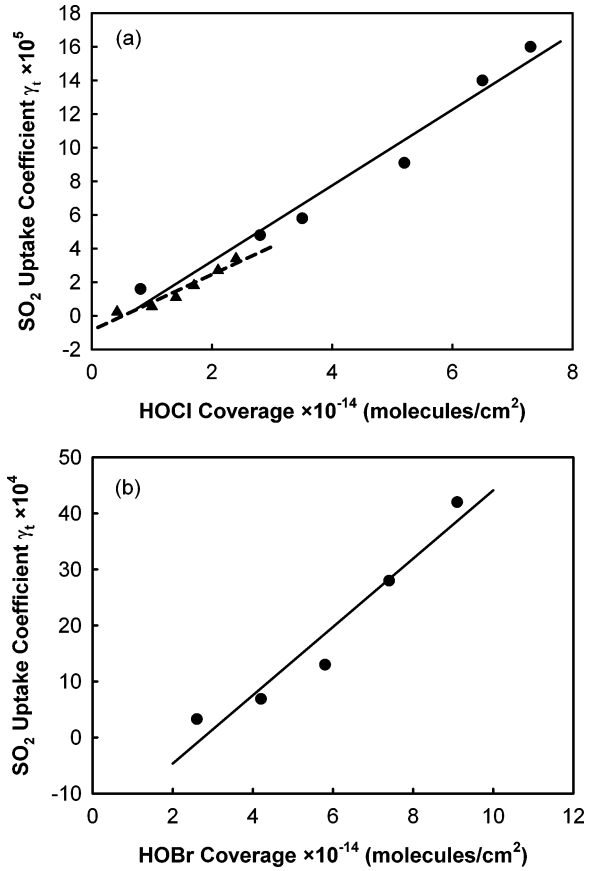

Figure 7. Plots of "true" uptake coefficients versus HOX coverage. (a) Relationship between the SO_2 true uptake coefficient, γ_t, and HOCl surface coverage at 190 K (●) and 210 K (▲). The lines are fitted to eq 12, and the slope of the fit is k_h. (b) Plot of the SO_2 true uptake coefficient, γ_t, versus the HOBr surface coverage at 190 K (●). The solid line is fitted to eq 12, and the slope of the fit is k_h. The fitted lines suggest that the uptake in the SO_2 reaction with either HOCl or HOBr on water-ice surfaces can be represented using the model outlined in the text. The plot also shows that the γ_t for the SO_2 reaction with HOBr is higher than the coefficient for the reaction with HOCl at a given surface coverage and 190 K. See text for details.

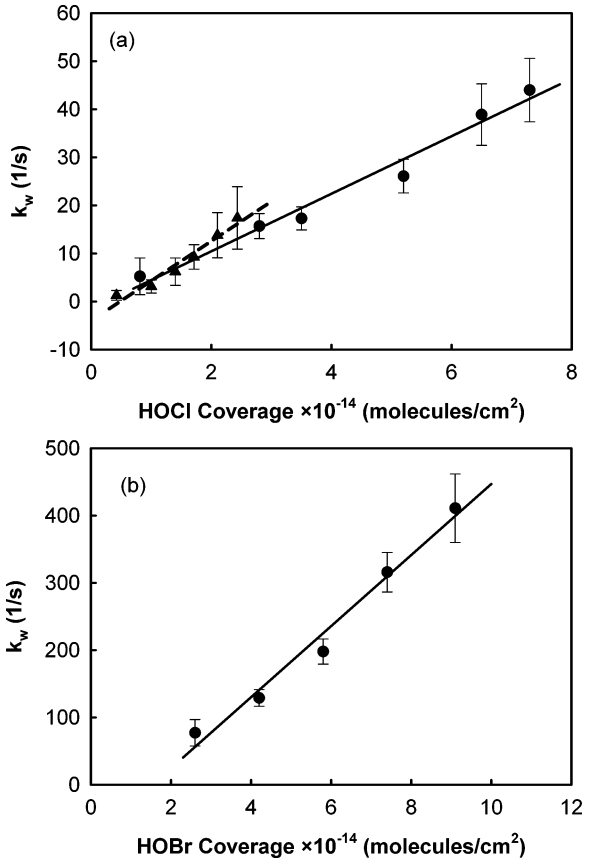

Figure 8. Plots of pseudo-first-order rate constants versus measured HOX coverage. (a) Relationship between the pseudo-first-order rate constant k_w and total HOCl surface coverage at 190 K (●) and 210 K (▲). The rate constant, k_h^2, was determined from the slope of the fit to be $(6.0 \pm 1.6) \times 10^{-14}$ molecules^{-1}·cm^2·s^{-1} and $(8.3 \pm 2.4) \times 10^{-14}$ molecules^{-1}·cm^2·s^{-1} at 190 and 210 K, respectively. (b) Relationship between the pseudo-first-order rate constant k_w and HOBr surface coverage at 190 K (●). The second-order rate constant was determined from the slope of the fit to be $(5.3 \pm 1.8) \times 10^{-13}$ molecules^{-1}·cm^2·s^{-1} at 190 K.

reaction with HOBr is higher than that with HOCl on ice surfaces for a given surface coverage and temperature. Equation 10 also can be expressed in terms of

$$\text{rate} = k_h^2 \theta_{HOX}^T P_{SO_2} \quad (13)$$

where k_h^2 is the second-order heterogeneous rate constant, which can be determined from a plot of k_w versus θ_{HOX}^T. A plot of k_w versus θ_{HOCl}^T is shown in Figure 8a, and a plot of k_w versus θ_{HOBr}^T is shown in Figure 8b. The rate constant k_h^2 of SO_2 reaction with HOCl was determined to be $(6.0 \pm 1.6) \times 10^{-14}$ and $(8.3 \pm 2.4) \times 10^{-14}$ molecules^{-1}·cm^2·s^{-1}, at 190 and 210 K, respectively; the rate constant $k_h^2$of SO_2 reaction with HOBr was $(5.3 \pm 1.8) \times 10^{-13}$ molecules^{-1}·cm^2·s^{-1} at 190 K.

The oxidation capability of hypobromite is weaker than that of hypochlorite, on the basis of emf (eqs 14 and 15). The present work shows that the rate of SO_2 reaction with HOBr on water-

$$HOBr + 2e^- \rightarrow Br^- + OH^- \qquad E_b^\circ = 0.766 \text{ V} \quad (14)$$

$$HOCl + 2e^- \rightarrow Cl^- + OH^- \qquad E_b^\circ = 0.890 \text{ V} \quad (15)$$

ice films is more rapid than that with HOCl (k_h^2(HOBr)/k_h^2(HOCl) = 9, or k_h(HOBr)/k_h(HOCl) = 26) at 190 K. Oxidation of S(IV) by HOX in aqueous solution has been studied; $k_{HOBr}{}^a = (5.0 \pm 1) \times 10^9$ M^{-1}s^{-1}, and $k_{HOCl}{}^a = 7.6 \times 10^8$ M^{-1}s^{-1} at 298 K.[25,27] Because these rate constants were determined under ambient conditions, we cannot make a direct quantitative comparison between the aqueous rate and the γ values obtained from the present study. However, it is clear that the same trend

applies, i.e., $k_{HOBr} > k_{HOCl}$. Reaction rates are affected by the pH in solutions. We assume that uptake coefficients are affected by the pH on the ice surfaces as well. The pK_a value of HOBr is ~8.8, and the pK_a value of HOCl is ~7.5 at 298 K.[25,27] This implies that [HOBr]/[OBr^-] > [HOCl]/[OCl^-] in a neutral or slightly acidic environment. For example, at pH = 7, [HOBr]/[OBr^-] = 120, and [HOCl]/[OCl^-] = 4.7. If we accept that the reaction between HOX/OX^- and SO_2 on ice is nucleophilic, analogous to the reaction in solution, we see that HOX, rather than OX^-, is the reactant ($k_{HOX} > k_{OX^-}$) at pH ~ 7, and we conclude that HOBr is more reactive than HOCl on the basis of the Lewis acid−base theory. Foelman et al.[25] proposed that a reaction intermediate for HOX reaction with SO_3^{2-} is HOX···SO_3^{2-} in solutions. We postulate that a reaction intermediate for the reaction of HOX + SO_2 on ice is **I**, and

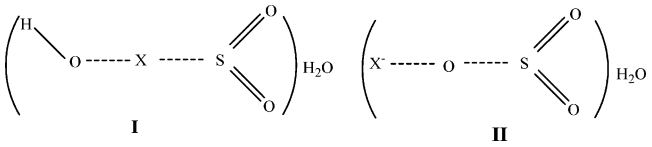

I **II**

X = Cl or Br

that a reaction intermediate for OX^- reaction with SO_2 is **II**.

We assume that the reaction intermediate is similar to that in solutions. S from SO_2 nucleophilically attacks the halogen atom in HOX, producing a good leaving group $OH^{\delta-}$. Presumably, the intermediate, HOX···SO_2, is hydrated on the ice surface to form $XSO_3^{\delta-}$. It is also possible that S attacks the oxygen atom of HOX, resulting in a more electrostatic repulsive intermediate with an $X^{\delta+}$ leaving group. $X^{\delta+}$ is a poor leaving group, so this is not a favorable pathway. For reaction of OX^- with SO_2, S nucleophilically attacks the oxygen atom of OX^- (**II**), producing a good leaving group X^-. This is an anticipated reaction pathway based on the chemical property of the leaving group.

At pH ~ 5.5−7, we have [HOX] > [OX^-] and k_{HOX}[HOX(ad)] ≫ k_{OX^-}[OX^-(ad)]; eq 9 can be simplified to

$$-\frac{d[SO_2(g)]}{dt} = k_{HOX}[HOX(ad)][SO_2(g)] \qquad (16)$$

This does not change the functional form of eq 12, but $\theta^T_{HOX} \approx \theta_{HOX}$. In other words, under neutral or slightly acidic conditions, dissociation of HOX on ice (eq 5) may be omitted, as we did in a previous publication.[34] The rate of the HOBr reaction with SO_2 is approximately an order of magnitude faster than that reaction with HOCl, because k_{HOBr}[HOBr(ad)] > k_{HOCl}[HOCl(ad)] at the same pH and HOX coverage.

We have demonstrated that heterogeneous reactions between HOX (X = Cl or Br) and SO_2 occur on the ice surface at 190 and 210 K. We can speculate that likely products are HSO_4^- and X^-, according to eqs 17 and 18, similar to the aqueous phase reactions. γ of HOX + X^- is larger than that of HOX +

$$HOX + SO_2 \xrightarrow[H_2O(s)]{k_7} H^+ + XSO_3^- \qquad (17)$$

$$XSO_3^- + H_2O(s) \xrightarrow{k_8} HX(s) + HSO_4^- \qquad (18)$$

$$HOX + HX(s) \xrightarrow{k_9} H_2O(s) + X_2 \qquad (19)$$

SO_2 on ice films.[31,42] This suggests that the rate-limiting step can be the reaction in either eq 17 or 18. Reactions occurring in the aqueous phase indicate that the rate-limiting step is that

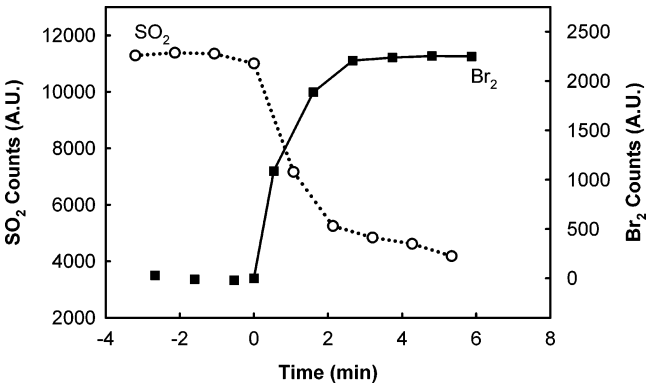

Figure 9. Possible products of the heterogeneous reaction of SO_2 + HOBr on ice surfaces at 190 K. A plot of the SO_2 loss versus the reaction time is shown on the left-hand *Y*-axis. The formation of Br_2, detected by QMS at $m/e = 158$, is shown on the right-hand *Y*-axis of the plot. The combination of plots suggests that a redox reaction is occurring between HOBr and SO_2, with potential products HSO_4^- and X^-. See text for details. The error bars are approximately the size of the plotted points.

depicted in eq 18.[27] If the reactions in eqs 17−19 correctly depict potential products on the water-ice surface, we should be able to detect Br_2 or Cl_2 in the gas phase.

Figure 9 shows both the formation of Br_2 and the loss of SO_2, for the reaction of HOBr + SO_2 on an ice surface at 190 K. The SO_2 signal is plotted on the left-side *Y*-axis, and the Br_2 signal is on the right-side *Y*-axis. The plot shows that the SO_2 signal decreases with the reaction time, and that Br_2, detected by the QMS at $m/e = 158$, is generated from the surface as the reaction proceeds. For the HOCl + SO_2 reaction on the ice surface at 190 K, the Cl_2 signal increase is weak, as detected by the QMS at $m/e = 70$. The Cl_2 signal intensity is not as strong as that of Br_2. Figure 9 shows that the reaction likely proceeds via intermediate **I**, and presumably either intermediates or reactants involve hydration steps, so that $BrSO_3^-$ is formed near the surface. Finally, $BrSO_3^-$ is converted to HSO_4^- and Br^-. The reaction between HOBr and Br^- produces Br_2. This also implies that if heterogeneous reactions of HOX + SO_2 occur on NaX-ice (X = Cl or Br), such as on the deliquescent sea-salt ice particles in the remote MBL, reaction HOX + X^- will take place first (eq 19).[49,50] HOX will probably be consumed on the NaX-ice surface first. Rates for the HOX + SO_2 reaction will be decreased, due to Br^- and Cl^- near the sea-salt particle surfaces reacting with HOX to reduce the effective surface coverage.

4.2. SO_2 Reaction with HOCl at Varying Temperature. The uptake coefficient for SO_2 reaction with HOCl on water-ice film decreases as the temperature increases from 190 to 238 K (Figure 5). This trend can be explained by the above model (eq 12 or 16). The temperature dependence of the initial uptake coefficient can be described using the Arrhenius equation, ln $\gamma_t \propto -E_a/RT$. The activation energy was determined from a plot of log γ_t versus $1/T$ (as shown in Figure 5) for the temperature range of 190−238 K. $E_a = -37 \pm 10$ kJ/mol. $\gamma_t = 3.4 \times 10^{-15} \exp(4.45 \times 10^3/T)$. The negative E_a suggests that the transition-state complex [HOCl···SO_2] is stabilized by the ice surface. The heat of uptake of HOCl on ice surfaces is approximately 35.5 ± 8.4 kJ/mol.[31] After the stabilization of transition-state complex by the ice is taken into consideration, the value $E_a = -37 \pm 10$ kJ/mol is reasonable. We also expect that $\Delta S^{\ddagger}$ is negative, because the transition-state complex is adsorbed on the surface.

4.3. Comparison with Previous Studies. There are no reported uptake coefficients for SO_2 + HOCl on ice in the

TABLE 4: Uptake Coefficients for the SO_2 on Ice Surfaces and Reaction with HOX Influenced by H_2O Vapor

temp (K)	P_{SO_2} (Torr)	P_{H_2O}[b] (Torr)	HOX uptake amount (molecules/cm^2)	k_s (1/s)	k_w (1/s)	γ_w
190.8 ± 0.2[a]	1.6×10^{-6}		0	0.65 ± 0.09	0.65 ± 0.10	$(4.4 \pm 0.6) \times 10^{-5}$
190.3 ± 0.3	1.4×10^{-6}	4.9×10^{-3}	0	2.0 ± 0.3	2.0 ± 0.3	$(1.3 \pm 0.2) \times 10^{-4}$
190.0 ± 0.4	1.4×10^{-6}	7.1×10^{-3}	0	3.6 ± 0.4	3.7 ± 0.4	$(2.4 \pm 0.3) \times 10^{-4}$
190.1 ± 0.4	1.4×10^{-6}	1.1×10^{-2}	0	4.2 ± 0.7	4.2 ± 0.7	$(2.9 \pm 0.3) \times 10^{-4}$
190.8 ± 0.2[a]	1.6×10^{-6}		3.3×10^{14} (HOBr)	3.1 ± 1.0	3.1 ± 1.0	$(2.1 \pm 0.7) \times 10^{-4}$
189.8 ± 0.7	1.6×10^{-6}	5.0×10^{-3}	$(3.0 \pm 0.5) \times 10^{14}$ (HOBr)	64.9 ± 12.9	78.2 ± 15.4	$(5.0 \pm 1.0) \times 10^{-3}$
190.3 ± 0.7	1.5×10^{-6}		$(2.0 \pm 0.3) \times 10^{14}$ (HOCl)	2.3 ± 0.5	2.3 ± 0.5	$(1.5 \pm 0.7) \times 10^{-4}$
190.1 ± 0.3	1.4×10^{-6}	4.9×10^{-3}	$(3.5 \pm 0.5) \times 10^{14}$ (HOCl)	16.8 ± 2.3	17.3 ± 2.4	$(1.2 \pm 0.2) \times 10^{-3}$
190[c]	1.4×10^{-6}	$\sim 10^{-3}$	2.0×10^{14} (HOCl)			7.3×10^{-4}

[a] Data are taken from ref 34. [b] Additional water vapor over the ice surface. [c] Calculated from Figure 3 at $\theta_{HOCl} = 2.0 \times 10^{14}$. P_{H_2O} varies slightly from experiment to experiment, typical $P_{H_2O} \leq 1 \times 10^{-3}$.

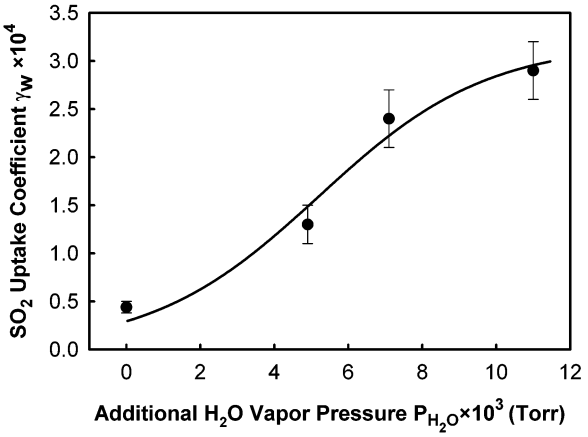

Figure 10. Relationship between the initial uptake coefficient of SO_2, γ_w, and presence of additional H_2O vapor on water-ice films at 190 K. The thickness of the ice film is 3.3 ± 0.2 μm. The partial pressure of SO_2 is $(1.4 \pm 0.2) \times 10^{-6}$ Torr, and the total pressure in the reactor is 1.000 ± 0.007 Torr. The plot shows that γ_w increases as the added H_2O-vapor pressure increases over the water-ice surface.

temperature range of 190−240 K. The reaction in the aqueous phase occurs under conditions very different from those studies here, and it is not possible to make a direct comparison.

We noted that the initial uptake coefficient γ_w value for the SO_2 reaction with HOBr under the concurrent flow condition is nearly 24-fold higher than the γ_w of SO_2 on HOBr-treated ice film at 190 K ($\theta_{HOBr} = (3.0 \pm 0.3) \times 10^{14}$ molecules/cm^2, Table 4).[34] We define this ratio as $(\gamma_w^{co-flow}/\gamma_w^{treated})_{HOBr} \approx 24$. One possible cause is additional water vapor in the flow reactor; this vapor was introduced into the reactor by bubbling He through the HOBr solution that was maintained at 273.15 K, to generate fresh ice surfaces and newly adsorbed HOBr that would be immediately available for reaction with SO_2 in the concurrent flow experiment. We conducted an experiment to examine the effect of additional water vapor on uptake of SO_2 on water-ice at 190 K. Figure 10 shows that the γ_w value of SO_2 on ice increases approximately 7-fold as the water vapor pressure increases from the saturation ice vapor pressure to 1.1×10^{-2} Torr. The experimental conditions are listed in Table 4. This pattern of increase suggests that either SO_2 adsorbs onto newly generated ice surfaces created by the water vapor or else water vapor adsorbs over the SO_2-adsorbed sites, so that additional SO_2 molecules can be further adsorbed on these sites. We also found that the γ_w of SO_2 reaction with HOCl on ice in the concurrent flow conditions is larger than that of SO_2 on HOCl-treated ice (see Table 4). The ratio of these two coefficients is expressed as $(\gamma_w^{co-flow}/\gamma_w^{treated})_{HOCl} \approx 8$. Because we established that the effect of surface deactivation on γ_w in the concurrent flow experiment is about 10−20% (cf. Figure 4), a reasonable explanation to the observed difference is that, in the HOCl-treated ice experiment, the ice vapor from the treated-HOCl ice surface is re-adsorbed on top of some adsorbed HOCl molecules during the time period in which the SO_2 flow and the QMS signal stabilize. The water vapor adsorbs on top of adsorbed HOCl effectively reduces HOCl surface coverage available for the reaction with SO_2, and results in a lower γ_w value. In the SO_2 and HOCl concurrent flow experiment, a freshly formed HOCl reactive site reacts with SO_2 readily and immediately. There is no reduction in the quantity of available HOCl sites. This explanation may also account for the observed differences in γ_w values between SO_2 on HOBr-treated ice surfaces and SO_2 reaction with HOBr on ice in the concurrent flow experiment. The ratio $(\gamma_w^{co-flow}/\gamma_w^{treated})_{HOBr}$ is higher than $(\gamma_w^{co-flow}/\gamma_w^{treated})_{HOCl}$. A possible explanation derives from the following observation. The heat of uptake of HOBr on ice is higher than that of HOCl on ice. This implies that the ice film, consisting of ice granules on a micrometer scale, is likely be annealed after HOBr molecules adsorb on the ice, thereby resulting in ice of a more dynamic nature. After the ice surface is treated by HOBr, increasing numbers of H_2O molecules can be re-adsorbed on HOBr sites, and the effective HOBr surface coverage becomes lower. Thus, $(\gamma_w^{co-flow}/\gamma_w^{treated})_{HOBr} > (\gamma_w^{co-flow}/\gamma_w^{treated})_{HOCl}$.

V. Conclusion

We have studied the heterogeneous reaction of SO_2 + HOX (X = Cl or Br) on ice surfaces using a low-temperature flow reactor coupled with a differentially pumped quadrupole mass spectrometer. The initial uptake coefficient γ_w was determined as a function of HOX coverage on ice film surfaces. γ_w for the SO_2 reaction with HOCl was determined to be in the range of $(3.5 \pm 2.5) \times 10^{-4}$ to $(3.0 \pm 0.5) \times 10^{-3}$ at 190 K, and $(8.2 \pm 6.6) \times 10^{-5}$ to $(1.1 \pm 0.4) \times 10^{-3}$ at 210 K. γ_w for SO_2 reaction with HOBr was determined to be in the range $(5.2 \pm 1.3) \times 10^{-3}$ to $(2.7 \pm 0.4) \times 10^{-2}$ at 190 K. The effect of temperature on the uptake coefficients for SO_2 reaction with HOCl was investigated, and the activation energy E_a was determined to be about −37 ± 10 kJ/mol at 190−238 K. The SO_2 uptake is discussed in terms of the Eley−Rideal mechanism. The present study suggests that SO_2 uptake is enhanced, due to reaction with HOX on ice, relative to SO_2 uptake on water-ice at 190 and 210 K; potential products of heterogeneous reaction of SO_2 + HOX on ice surfaces are X^- (X = Cl or Br) and HSO_4^-. SO_2 reaction with HOBr is faster than the analogous reaction with HOCl on ice surfaces at 190 and 210 K. However, the γ_w of SO_2 reaction with HOCl on ice at the MBL temperature (≥230 K) is comparable with the γ_w of SO_2 on water-ice. Thus, SO_2 oxidation by HOCl should not be a significant pathway in the MBL.

Acknowledgment. This work was supported by the National Science Foundation under grant ATM-0355521.

References and Notes

(1) Solomon, S.; Garcia, R. R.; Rowland, F. S.; Wuebbles, D. J. *Nature* **1986**, *321*, 755.
(2) Tolbert, M. A.; Rossi, M. J.; Malhotra, R.; Golden, D. M. *Science* **1987**, *238*, 1258.
(3) Molina, M. J.; Tso, T. L.; Molina, L. T.; Wang, F. C. Y. *Science* **1987**, *238*, 1253.
(4) Foster, K.; Plastridge, R. A.; Bottenheim, J. W.; Shepson, P. B.; Finlayson-Pitts, B. J.; Spicer, C. W. *Science* **2001**, *291*, 471.
(5) Singh, H. B.; Gregory, G. L.; Anderson, B.; Browell, E.; Sachse, G. W.; Davis, D. D.; Crawford, J.; Bradshaw, J. D.; Talbot, R.; Blake, D. R.; Thornton, D.; Newell, R.; Merrill, J. *J. Geophys. Res.* **1996**, *101*, 1907.
(6) Platt, U.; Moortgat, G. K. *J. Atmos. Chem.* **1999**, *34*, 1.
(7) Graedel, T. E.; Keene, W. C. *Global Biogeochem. Cycle* **1995**, *9*, 47.
(8) Barrie, L. A.; Hoff, R. M. *Atmos. Environ.* **1984**, *18*, 2711.
(9) Jobson, B. T.; Niki, H.; Yokouchi, Y.; Bottenheim, J.; Hopper, F.; Leaitch, R. *J. Geophys. Res.* **1994**, *99*, 25355.
(10) Keene, W. C.; Sander, R.; Pszenny, A. A. P.; Vogt, R.; Crutzen, P. J.; Galloway, J. N. *J. Aerosol Sci.* **1998**, *29*, 339.
(11) Seinfeld, J. H.; Pandis, S. N. *Atmospheric Chemistry and Physics*; Wiley: New York, 1998; Chapters 6 and 19.
(12) Colin, J. L.; Renard, D.; Lescoat, V.; Jaffrezo, J. L.; Gros, J. M.; Strauss, B. *Atmos. Environ.* **1989**, *23*, 1487.
(13) Tranter, M.; Brimblecombe, P.; Davies, T. D.; Vincent, C. E.; Abvehams, P. W.; Blackwood, I. *Atmos. Environ.* **1986**, *20*, 517.
(14) Krischke, U.; Staubes, R.; Brauers, T.; Gautrois, M. Burkert, J.; Stöbener, D.; Jaeschke, W. *J. Geophys. Res.* **2000**, *105*, 14413.
(15) Valdez, M. P.; Bales, R. C.; Stanley D. A.; Dawson G. A. *J. Geophys. Res.* **1987**, *92*, 9779.
(16) Hoppel, W.; Pasternack, L.; Caffrey, P.; Frick, G.; Fitzerald, J.; Hegg, D.; Gao, S.; Ambrusko, J.; Albrechcinski, T. *J. Geophys. Res.* **2001**, *106*, 27575.
(17) Choi, J.; Conklin, M. H.; Bales, R. C.; Sommerfeld, R. A. *Atmos. Environ.* **2000**, *34*, 793.
(18) Diehl, K.; Mitra, S. K.; Pruppacher, H. R. *Atmos. Res.* **1998**, *47*−*48*, 235.
(19) Sommerfeld, R. A.; Lamb, D. *Geophys. Res. Lett.* **1986**, *13*, 349.
(20) Conklin, M. H.; Bales, R. C. *J. Geophys. Res.* **1993**, *98*, 16851.
(21) Conklin, M. H.; Sommerfeld, R. A.; Laird, S. K.; Villinski, J. E. *Atmos. Environ.* **1993**, *27A*, 159.
(22) Mitra, S. K.; Barth, S.; Pruppacher, H. R. *Atmos. Environ.* **1990**, *24A*, 2307.
(23) Chu, L.; Diao, G. W.; Chu, L. T. *J. Phys. Chem. A* **2000**, *104*, 7565.
(24) Clegg, S. M.; Abbatt, J. P. D. *Atmos. Chem. Phys.* **2001**, *1*, 73.
(25) Foelman, K. D.; Walker, D. M.; Margerum, D. W. *Inorg. Chem.* **1989**, *28*, 986.
(26) Hartz, K. E. H.; Nicoson, J. S.; Wang, L.; Margerum, D. W. *Inorg. Chem.* **2003**, *42*, 78.
(27) Troy, R. C.; Margerum, D. W. *Inorg. Chem.* **1991**, *30*, 3538.
(28) Vogt, R.; Crutzen, P. J.; Sander, R. *Nature* **1996**, *383*, 327.
(29) Keene, W. C.; Sander, R.; Pszenny, A. A. P.; Vogt, R.; Crutzen, P. J.; Galloway, J. N. *J. Aerosol Sci.* **1998**, *29*, 339.
(30) von Glasow, R.; Sander, R.; Bott, A.; Crutzen, P. J. *J. Geophys. Res.* **2002**, *107*, 4323.
(31) Chu, L.; Chu, L. T. *J. Phys. Chem. A* **1999**, *103*, 691.
(32) Impey, G. A.; Shepson, P. B.; Hastie, D. R.; Barrie, L. B.; Anlauf, K. G. *J. Geophys. Res.* **1997**, *102*, 16005.
(33) Impey, G. A.; Mihele, C. M.; Anlauf, K. G.; Barrie, L. A.; Shepson, P. B. *J. Atmos. Chem.* **1999**, *34*, 21.
(34) Jin, R.; Chu, L. T. *J. Phys. Chem. A* **2006**, *110*, 3647.
(35) Chu, L. T.; Heron, J. W. *Geophys. Res. Lett.* **1995**, *22*, 3211.
(36) Chu, L. T. *J. Vac. Sci. Technol. A.* **1997**, *15*, 201.
(37) Keyser, L. F.; Leu, M.-T. *J. Colloid Interface Sci.* **1993**, *155*, 137.
(38) D'Ans, J.; Freund, H. E. Z. *Elektrochem.* **1957**, *61*, 10.
(39) Chu, L. T.; Leu, M.-T.; Keyser, L. F. *J. Phys. Chem.* **1993**, *97*, 12798.
(40) Toth, Z.; Fabian, I. *Inorg. Chem.* **2004**, *43*, 2717.
(41) Fickert, S.; Adams, J. W.; Crowley, J. N. *J. Geophys. Res.* **1999**, *104*, 23719.
(42) Chu, L.; Chu, L. T. *J. Phys. Chem. A* **1999**, *103*, 8640.
(43) Brown, R. L. *J. Res. Natl. Bur. Stand. (U. S.)* **1978**, *83*, 1.
(44) Cussler, E. L. *Diffusion, Mass Transfer in Fluid Systems*; Cambridge University Press: New York, 1984; Chapter 4.
(45) Chu, L.; Chu, L. T. *Recent Res. Devel. Geophys.* **2000**, *3*, 141.
(46) Keyser, L. F.; Moore, S. B.; Leu, M.-T. *J. Phys. Chem.* **1991**, *95*, 5496.
(47) Keyser, L. F.; Leu, M.-T. *Microscopy Res. Technique* **1993**, *25*, 343.
(48) Keyser, L. F.; Leu, M.-T.; Moore, S. B. *J. Phys. Chem.* **1993**, *97*, 2800.
(49) Huff, A. K.; Abbatt, J. P. D. *J. Phys. Chem. A* **2002**, *106*, 5279.
(50) Chu, L. T.; Diao, G. W.; Chu, L. *J. Phys. Chem. A* **2002**, *106*, 5679.